Journal of Materials Chemistry C

Accepted Manuscript

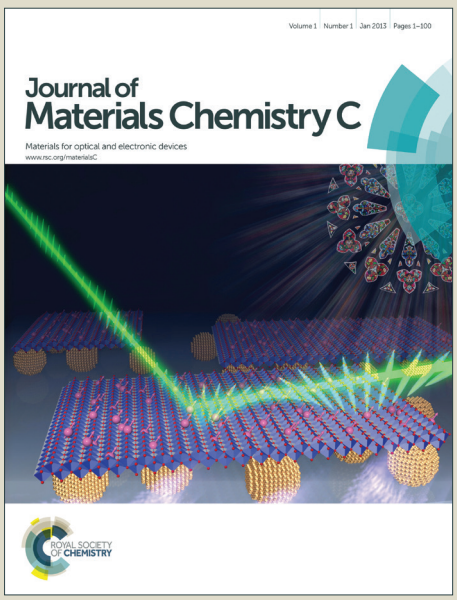

ROYAL SOCIETY OF CHEMISTRY

www.rsc.org/materialsC

Journal Name

RSCPublishing

ARTICLE

Photochemical synthesis of pyrene perfluoroalkyl derivatives and their embedding in a polymethylmethacrylate matrix. A spectroscopic and structural study.

Cite this: DOI: 10.1039/xoxxoooooox

Received ooth January 2012,
Accepted ooth January 2012

DOI: 10.1039/xoxxoooooox

www.rsc.org/

I. Pibiri,[a,b,*] S. Buscemi,[a] A. Palumbo Piccionello,[a,b] M. L. Saladino,[a,*] D. Chillura Martino[a,c] and E. Caponetti.[a,d]

ABSTRACT: A photochemical, alternative and eco-compatible approach to perfluoroalkyl derivatives of pyrene is presented. The perfluoroalkyl chain is regiospecifically introduced at the 1 position of pyrene. The synthesized products have been embedded in a polymethylmethacrylate matrix by photocuring at 365nm. Both the photochemical reactions can be considered a "green tool" for the synthetic chemist in order to obtain materials with perspective optoelectronic applications. The so-obtained composites have been the object of a study by UV and Fluorescence Spectroscopy in order to explore their luminescence properties. The Small Angle X-ray Scattering and the Transmission Electron Microscopy techniques were used to investigate the microstructure. A correlation between the optical and the structural properties is herein presented.

Introduction

Replacing inorganic semiconductors with organic materials is a strategy worth to consider in order to decrease manufacturing costs and allow production of lightweight and plastic substrates devices.

The physical-chemical properties of organic materials such as energy gap, solubility, electron affinity and air-stability can be finely tuned by small variations in the structure or composition providing a great level of flexibility in materials design.

In the context of design of materials for electronic and/or optical applications, pyrene is very attractive for its peculiar electronic and photophysical properties. It is a blue-light-emitting chromophore, based on a large conjugated aromatic system, with good chemical stability and high photoluminescence efficiency.[1] It finds its major application as a fluorescence probe,[2-4] but it has also high charge carrier mobility and excellent hole injection ability compared to other chromophores.[5]

Due to their unique properties pyrene and its analogues and derivatives have received great deal of attention, inspiring researchers from various scientific fields to study their possible application, in particular as Organic Light-Emitting Diodes (OLEDs), Organic Field-Effect Transistors (OFETs) and Organic Photovoltaic (OPV) such as bulk heterojunction and dye sensitized solar cells.[1,5-7]

The development of new synthetic routes to substituted pyrene will allow and promote the expansion of pyrene as a building block for organic electronics.

In this context, many attempts to modify the molecular structure of pyrene have been made in order to enhance its electronic and optical properties, by introducing specific electron-donating or -accepting groups at the pyrene ring.[1]

In particular, one of the design motifs for air-stable n-type rylene-based semiconductor materials was to incorporate strong electron-withdrawing groups, in order to get high-lying energy level of the highest occupied molecular orbitals (HOMO), to facilitate both hole injection and transport. Core-cyanated, core-fluorinated and N-fluoroalkylated perylene and naphthalene derivatives have been reported to exhibit high n-type mobility and air stability.[8-9]

In this context, perfluoroalkylated compounds, since the electron-withdrawing character of the R_F chain, in combination with their superb thermal stability, good solubility in various organic solvents, stability in air and to moisture or aggressive chemical environment, are excellent candidates for various practical applications, in particular materials to be used in electronic devices and for energy conversion.[10]

Moreover, perfluoroalkylated-pyrene derivatives are worth *per se*, e.g. for application as fluorescence probe in contexts in which the presence of a perfluoroalkylated moiety would be helpful, as for affinity to the analyzed materials or to improve the solubility of pyrene in fluorinated media,[11-13] or when the hydrophobic association of fluorinated surfactants cannot be monitored by pyrene.[14]

Although many efforts have been made to direct C-H functionalization,[15] also making use of metal catalyst,[16-21] approaches to the direct perfluoroalkylation of polycyclic aromatics remain highly desirable in terms of atom and step economy and direct C-H bond transformation of unreactive arenes is still a challenge.

Li et al. have recently reported direct functionalization of electron-deficient and electron-rich polycyclic aromatics *via* copper mediated radical perfluoroalkylation.[22]

A great variety of perfluoroalkylated polycyclic aromatics, such as naphthalene, pyrene, and perylene, can be prepared *via* this method with high yields.

Radical perfluoroalkylation as addition to alkenes or aromatic substitution with perfluoroalkyl iodides are well-known thermal processes.[23,24]

Nevertheless, the photochemical approach, despite its great potential, is still a limitedly explored synthetic methodology.[10,25]

Pyrene functionalization may allow both the control of the molecular packing, and the fine-tuning of the optical properties.

Nowadays, the possibility to embed small molecules with defined properties in a polymeric matrix has to be considered a useful tool of choice for the fabrication of high-performance devices.

Polymer-based composites have been studied extensively due to their lightweight, ease of manufacture and due to the fact that a polymer in the presence of a filler can change its physico-chemical properties including transparency, mechanical and thermo-chemical stability.[26-28] The preparation of new transparent and luminescent composites consisting of polymers as matrix and emitters as fillers is one of the objectives for the development of OLEDs, lasers and solar cells.[29]

Polymethylmethacrylate (PMMA) is a common plastic polymer that has been commercially used for many years in various sectors, such as ophthalmology, orthopedics and consolidation of mural paintings; it has been used to incorporate macromolecules such as bis-azopyrrolidine linked by an ethylenglycol chain and in the production of films with hydrophobic properties. In our opinion, PMMA is an excellent candidate in the realization of electronic devices due to its high dielectric constant, low water permeability, good electrical resistivity, transparency and ductility.[30,31]

In the frame of our on-going studies on the photoreactivity of organic compounds[32-40] we decided to explore the photo-perfluoroalkylation of pyrene. The pyrene derivatives, hence, have been used for the preparation of pyrene-PMMA composites by photocuring.[41-43] The luminescence properties and the microstructure of the so-formed composites have been studied by Fluorescence Spectroscopy, SAXS and TEM techniques, respectively.

Experimental

Materials and Methods

All solvents and reagents were purchased by Aldrich.

Methylmethacrylate (MMA) was purified using a disposable column to eliminate the polymerization inhibitor.

Preparation Methodologies.

Preparation of perfluoroalkylated products. Preliminary irradiations of pyrene **1** in the presence of C_4F_9I were performed in a Rayonet apparatus with 35W Hg lamps at different wavelengths (254, 305 or 365 nm) and in different kinds of solvents, such as acetonitrile (aprotic polar), methanol (protic polar), cyclohexane (apolar), and were monitored in a time span of 20h, screening the reaction conditions by TLC. The formation of photoproducts was observed in every medium and at every wavelength, but the reaction proceeds quickly at 254 nm. Concerning the solvent, in cyclohexane the reaction goes on slowly and in both cyclohexane and acetonitrile the formation of some amounts of photo-degradation products was observed. Moreover, the reaction was performed with different amounts of perfluoroalkylating reagent (1, 3, 10 equivalents) concluding that an excess of reagent (10 eq.) is necessary to get good photo-conversions.

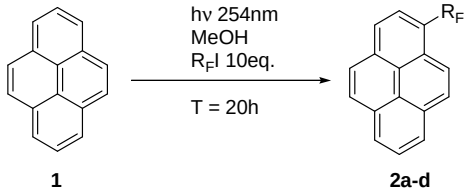

1 **2a-d**

	R_F	Yield%	SM recovered%	Yield on converted%
2a	C_4F_9	33	50	66
2b	C_6F_{13}	39	41	66
2c	C_8F_{17}	48	42	83
2d	$C_{10}F_{21}$	51	40	85

Scheme 1.

General procedure for the photochemical synthesis of compounds 2a-d. Photochemical reactions were carried out in anhydrous solvent by using a Rayonet RPR-100 photoreactor fitted with 16 Hg lamps irradiating at 254nm (in 45 mL Quarz vessels) and a merry-go-round apparatus. A sample of pyrene (0.35 g) in CH_3OH (350 mL) was apportioned into nine quartz tubes. After N_2 purging, the appropriate perfluoroalkyl Iodide (10eq.) was added and the solutions were irradiated for 20h. The solvent was removed under vacuum and chromatography of the residue returned starting material and gave **2a-d**, with yields (based on recovery of starting material) ranging from 66 to 85% (see Scheme 1).

1-(1,1,2,2,3,3,4,4,4-nonafluorobutyl)pyrene (**2a**)
(240 mg); white solid (precipitated by Petroleum 40-60°C), m.p. 90-92°C, ^{1}H NMR ($CDCl_3$, δ): 8.50 (br d, 1H), 8.27-8.21 (m, 6H), 8.13-8.08 (m, 2H); MS (*m/z*): 420 ([M]$^+$, 25), 251 (100), 201 (10), 125 (25), 100 (15).

1-(1,1,2,2,3,3,4,4,5,5,6,6,6-tridecafluorohexyl)pyrene (**2b**)
(350 mg); white solid (precipitated by Petroleum 40-60°C), m.p. 115-117°C, ^{1}H NMR ($CDCl_3$, δ): 8.50 (br d, 1H), 8.29-8.20 (m, 6H), 8.13-8.06 (m, 2H) ; MS (*m/z*): 520 ([M]$^+$, 20), 251 (100), 201 (10), 125 (20), 100 (10).

1-(1,1,2,2,3,3,4,4,5,5,6,6,7,7,8,8,8-heptadecafluorooctyl)pyrene (**2c**), (432 mg); white solid (precipitated by Petroleum 40-60°C), m.p. 149-152°C, ^{1}H NMR ($CDCl_3$, δ): 8.50 (br d, 1H), 8.30-8.21 (m, 6H), 8.13-8.08 (m, 2H) ; MS (*m/z*): 620 ([M]$^+$, 25), 251 (100), 201 (10), 126 (20), 44(80).

1-(1,1,2,2,3,3,4,4,5,5,6,6,7,7,8,8,9,9,10,10,10-henicosafluorodecyl)pyrene (**2d**), (635 mg); white solid (precipitated by Petroleum 40-60°C), m.p. 154-156°C, ^{1}H NMR ($CDCl_3$, δ): 8.50 (br d, 1H), 8.32-8.21 (m, 6H), 8.15-8.10 (m, 2H); MS (*m/z*): 720 ([M]$^+$, 15), 281 (10), 251 (100), 201 (10), 126 (20), 44(30).

Compounds **2a-b**[44] and **2c**[22] have physical characteristics identical to the compounds prepared by alternative procedures as reported in the literature.
This procedure is direct and clean, without formation of secondary photochemical products, due to the greater stability of the perfluoroalkylated products with respect to the parent compounds. This was further proved by the irradiation of the perfluoroalkylated products in the same reaction conditions that showed no formation of di- or poly-perfluoroalkylated derivatives nor photo-degradation products, as confirmed by TLC and GC-MS analysis.
The proposed photochemical procedure is more eco-compatible than that reported in the literature, which makes use of DMSO as solvent, high temperatures, and metal catalyst.[22,44]

Preparation of composites. The composites were prepared using the *in situ* polymerization method which was previously used to obtain several PMMA nanocomposites.[41-43] Pyrene and the photosynthesized products have been added at various molar concentration (see Table 1) to methylmethacrilate (MMA) monomer.
Compounds **1, 2a-d** were placed in 2 mL pyrex vials and dissolved in MMA by ultrasound (10 minutes), then 2,2-diethoxyacetophenone was added to start the photocuring process and the vials were irradiated at 365 nm in a Rayonet reactor equipped with eight 35W Hg lamps for at least 3h, up to complete photocuring.

Table 1. Concentration (mol/L) of the perfluoroalkylated compounds in PMMA composites.

1/PMMA	2a/PMMA	2b/PMMA	2c/PMMA	2d/PMMA
			$1\cdot10^{-5}$	
			$1\cdot10^{-4}$	
$2.33\cdot10^{-2}$			$1\cdot10^{-3}$	$1\cdot10^{-3}$
$4.65\cdot10^{-2}$	$2.3\cdot10^{-2}$	$1.8\cdot10^{-2}$	$1.5\cdot10^{-2}$	
$9.31\cdot10^{-2}$	$4.48\cdot10^{-2}$	$3.6\cdot10^{-2}$	$3.2\cdot10^{-2}$	$3\cdot10^{-2}$
$1.72\cdot10^{-1}$	$8.9\cdot10^{-2}$	$7.23\cdot10^{-2}$	$6.4\cdot10^{-2}$	
$3.71\cdot10^{-1}$				

The obtained composites, transparent and light yellowish solids, were cut and lapped to obtain discs of 1 cm in diameter and 2 mm in thickness. For the sake of comparison, pure PMMA was prepared following the same procedure (see Figure 1).

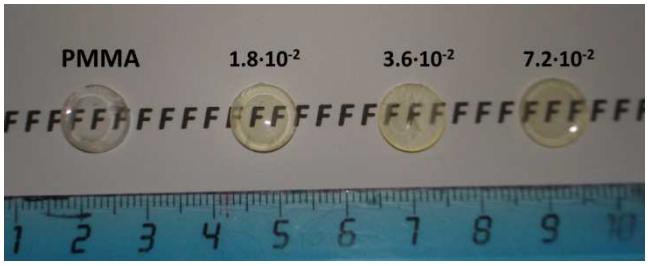

Figure 1. Pure PMMA and **2b/PMMA** composites.

Characterization Methods.
Melting points were determined by a Reichart-Thermovar hot-stage apparatus and are uncorrected.
Mass spectra have been registered by a GC-MS Shimadzu QP-2010.
^{1}H NMR spectra were recorded by a BRUKER 300 Avance spectrometer, operating at 300 MHz, with TMS as an internal standard.
Column chromatography was performed by using Flash silica gel (Merck, 0.040–0.063 mm) and Petroleum (fraction boiling in the range of 40–60 °C) as eluent.
The Emission spectra were acquired by using a Fluoromax 4 Horiba Jobin Yvon spectrofluorimeter. Samples, placed at 45°, were excited by a Xe source operating at 150W and a wavelength of 300nm; all the spectra shown in figures 2-5 have been registered by using the same operative instrumental conditions and parameters.
The chromaticity coordinates were calculated from the emission spectra using the Origin 8.0 software following the standard CIE 15:2004.
SAXS measurements were performed by using a Bruker AXS Nanostar-U instrument whose source was a Cu rotating anode working at 40kV and 18mA. The X-ray beam was monochromatized at a wavelength λ of 1.54 Å (Cu Kα) using a couple of Göbel mirrors and was collimated using a series of three pinholes with diameters of 500, 150 and 500μm. Samples were directly mounted on the sample stage to avoid additional scattering of the holder. Data were collected at room

temperature for 1000 sec by using a two-dimensional multiwire proportional counter detector placed at 24cm from the sample allowing the collection of data in the scattering vector ($Q= 4\pi\sin\theta/\lambda$) range 0.02–0.78Å^{-1}. The measurements were repeated in two portions of each sample to check its homogeneity.

TEM micrographs were acquired using a JEM-2100 (JEOL, Japan) electron microscope operating at 200kV accelerating voltage.

100 nm thick slices, prepared by using a Leica EM UC6 ultra-microtome, were put onto a 3 mm Cu grid "lacey carbon" for analysis.

Thermo-gravimetry analysis (TGA) was performed in nitrogen using a Q5000 IR apparatus from room temperature up to 600°C at a heating rate of 10°C/min. Once the final temperature was reached, specimens were left to cool down.

Results and discussion

The perfluoroalkylated derivatives of pyrene, dissolved in CH_3OH and in MMA, and the PMMA composites were the object of a study by UV (see Supporting Information Figure S1) and Fluorescence Spectroscopy in order to explore their luminescence (PL) properties. As an example, some representative emission spectra are reported in Figures 2 and 3.

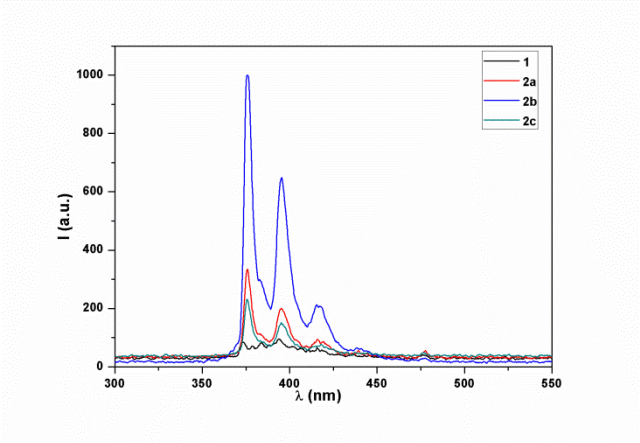

Figure 2. Emission spectra of 10^{-5} M pyrene (**1**) and perfluoroalkyl-derivatives **2a**, **2b**, and **2c** in CH_3OH.

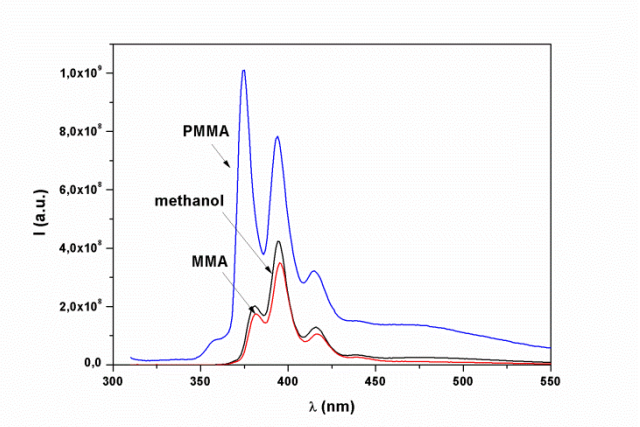

Figure 3. Emission spectra of 10^{-3}M **2c** in CH_3OH, MMA and PMMA.

The calculated fluorescence quantum yield and the energy gap relative to the first excited state are reported in Table 2 (see also Supporting Information Figure. S2).

Table 2. Emission Quantum Yields (ΦE) and singlet energy (E0-0, kJ/mol) for compounds **1** and **2a-d** in CH_3OH, MMA and PMMA.

	1	**2a**	**2b**	**2c**	**2d**
ΦE	0.72[a]	0.5[b]	1[b]	0.6[b]	-
E0-0(CH_3OH)	321[a]	328	324	328	-
E0-0(MMA)	-	-	-	330	-
E0-0(PMMA)	343	330	330	326	324

[a]lit. M. Montalti, A. Credi, L. Prodi, M.T. Gandolfi, Handbook of photochemistry, CRC – Taylor & Francis Ed.
[b] calculated by using pyrene as standard

The emission of the perfluoroalkyl-derivatives, in all medium, differs both in shape and in intensity from pyrene. The spectra of the derivatives lack the fine-structure peculiar of pyrene and they are blue-shifted. At concentration 10^{-5} M in CH_3OH the emission is more intense than that of pyrene (see Figure 2). Its value increases with concentration up to 10^{-3} M where the resulting emission was lower probably due to a quenching effect (see Figure 4).

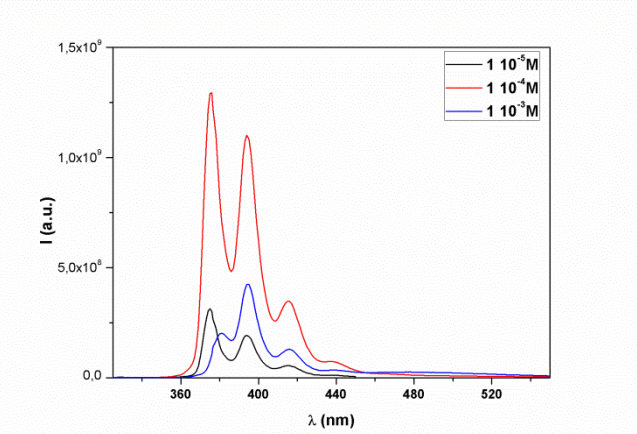

Figure 4. Emission spectra of **2c** in CH_3OH at three concentration.

Emission spectra for compounds **2a** and **2b** in acetonitrile have been already reported.[45] The authors claim that, respect to pyrene solution, the excimer emission was detectable only for concentration $1.3\cdot10^{-2}$M. The disfavored excimer formation in fluorinated systems, compared to pyrene or 1-methylpyrene, was ascribed to an electronic effect, that also causes a blue shift of the emission bands.[45] The more difficult formation of excimers may be due to the fluorophobic aggregation of the perfluorinated chains[46-48] that, at some concentration, can hinder the π-π stacking .[49]

The perfluoroalkyl-derivatives emit slightly less in MMA than in methanol solutions (see Figure 3). The emission trends of the PMMA composites is always similar to the one observed for solutions (see Figure 5). The emission intensity increases with

concentration without quenching effects. It has to be underlined that at 10^{-3}M the composites emission is stronger compared to CH_3OH solution.
At higher concentration the appearance of the excimer band at ~472nm was observed (see Figure 5).

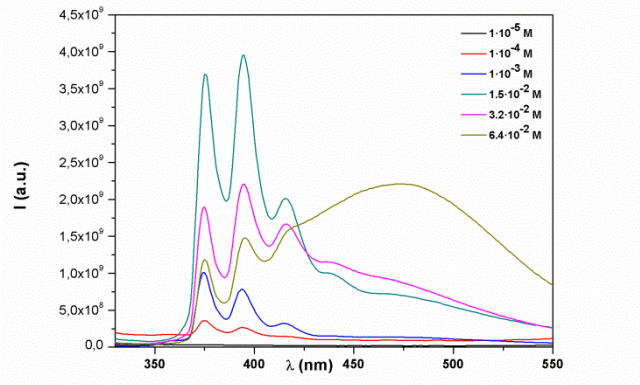

Figure 5. Emission spectra of the **2c/PMMA** composites as function of concentration.

In addition, on increasing the concentration, a change in the ratio between the intensities of the bands at 375 (I) and 394 nm (II) was observed (I_I/I_{II} see Figure 6). This change can be attributed to the association of some molecules. The observed behavior could be justified as some vibrational energy loss due to a proximity effect, that causes the emission from the lower vibrational band of the excited state more probable.

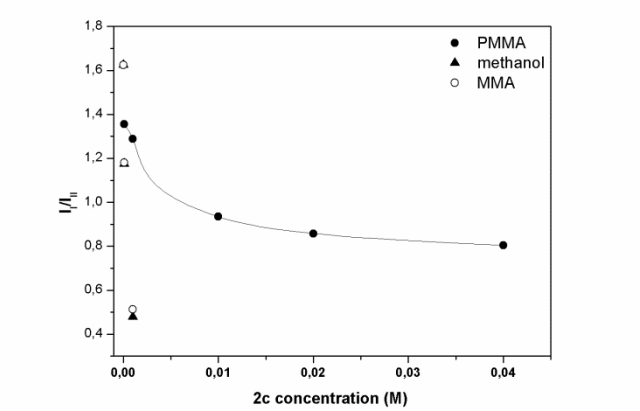

Figure 6. Dependence of the fluorescence intensity ratio of the first to the second vibronic bands (I_I/I_{II}) on the concentration of **2c** in PMMA composites, in CH_3OH and MMA solutions.

The I_I/I_{II} ratio is always lower in solution compared to the solid dispersion, as the loss of vibrational energy in solution is more consistent due to solvation effects of the medium, while, in contrast, in the solid phase, the molecules are somewhat frozen.
The photoluminescence of the composites is reported in Figure 7: there is no emission from the PMMA polymer (A in Figure 7), by embedding pyrene (B and C in Figure 7) there is a fair to good blue-violet emission. At a comparable concentration, **2a/PMMA** composites show a higher emission. For the more concentrated composite a notable shift of the emission to the white-greenish region was observed, confirming the formation of higher wavelenght emitting excimers, as indicated from fluorescence data.

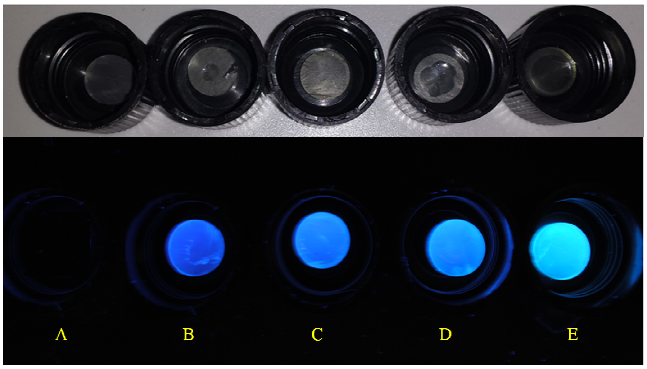

Figure 7. Photoluminescence of A) PMMA, B) $2.33\cdot10^{-2}$M **1/PMMA**, C) $9.31\cdot10^{-2}$M **1/PMMA**, D) $2.30\cdot10^{-2}$M **2a/PMMA**, E) $8.90\cdot10^{-2}$M **2a/PMMA**.

The chromaticity coordinates, calculated from the emission spectra, of the 2c/PMMA composites are reported in the Commission Internationale de l'Eclairage (CIE) chromaticity diagram (Figure 8)

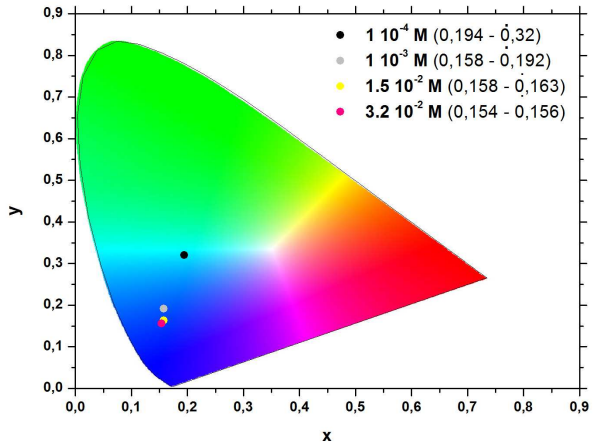

Figure 8. Chromaticity coordinates of the **2c/PMMA** composites.

The calculation of the CIE (x, y) coordinates of the **2c/PMMA** composites at concentration $1\cdot10^{-5}$ M was impossible due to the very weak emission. The CIE (x, y) coordinates of the **2c/PMMA** composites at higher concentration are located in the blue region, which further confirm that the emission is covering the blue-violet to green light region. Additionally, it is noteworthy that the emission of **2c/PMMA** composites at concentration $1\cdot10^{-4}$ M is located at the edge of the green region. On the other hand, the calculation of the CIE (x, y) coordinates of the **2c/PMMA** composites at concentration $6.4\cdot10^{-2}$M is affected by an high error, due to the contribute at

550 nm of the excimer emission, and the obtained CIE (x, y) coordinates are not considered reliable.

The chromaticity coordinates of the **1/PMMA**, **2a/PMMA**, **2b/PMMA** and **2d/PMMA** composites are reported in the Supporting Information Figure. S3-S6. No large differences were observed for the other composites, which CIE (x, y) coordinates are also located in the blue region.

SAXS measurements were performed on perfluoroalkyl-derivatives solutions and on PMMA composites to shed light on the structure of microdomains.

The acquired data on solution at various composition as well as some of those acquired on the composites show well defined peaks. Experimental intensities of **2c** in CH3OH and MMA, after corrections for the background and for the samples thickness, are reported vs. Q in Figure 9.

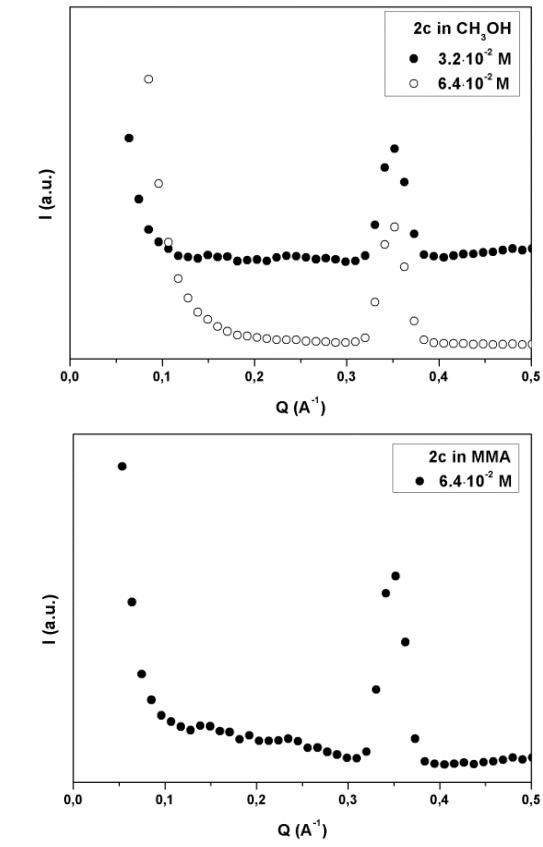

Figure 9. SAXS intensities vs scattering vector Q of **2c** in CH_3OH and MMA respectively.

The observed peaks in all scattering patterns indicate the formation of aggregates in solutions. The peak position does not change neither with concentration nor with the solvent. The corresponding aggregate size is ca. 18 Å. By comparing the SAXS pattern of the pure PMMA with that related to the **2c/PMMA** composite (see Figure 10), a peak corresponding to a repeating distance of ca. 19Å indicates the presence of structures similar to those present in solution. These structures are observed also for the **2d/PMMA** composites, but not for the **1/, 2a/** and **2b/PMMA** composites, indicating that the length of the fluorinated chain determine the tendency to aggregation. Moreover, SAXS data of the **2d/PMMA** evidence the presence of an additional peak at shorter Q-value. A repeating distance of ca. 21 and ca. 41 Å was evaluated from the two peaks position.

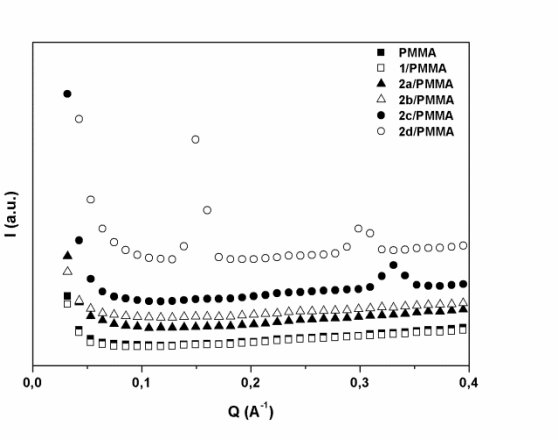

Figure 10. SAXS intensities vs scattering vector Q of pure PMMA and the composites at a concentration 3.2 10^{-2}M.

These findings indicate that the structure in the composites has to be attributed to perfluoroalkyl-derivative aggregation and could be consistent with a lamellar organization, as reported in the literature.[50] A notional pictorial image of the aggregate formation for **2c** is reported in Figure 11.

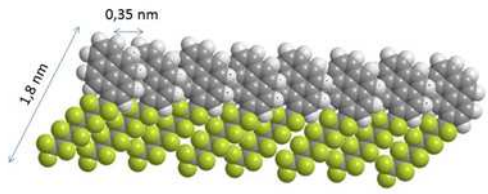

Figure 11. Notional pictorial representation of molecular organization for **2c**

The evaluated distance for the **2c/PMMA** composite is roughly corresponding to the molecule length. Notwithstanding, it is still unclear why the **2c/PMMA** does not display a more intense peak at longer distances (lower Q-values) as the **2d/PMMA** does. Therefore, a 6.4 10^{-2} M **2c/PMMA** composite was analyzed. SAXS data, reported in supporting information (see Figure S7), are characterized by the presence of two peaks corresponding to a repeating distance of ca. 18 and ca. 41 Å. This indicates that the organization in the sample is concentration dependent and, more important, that the two

peaks cannot be ascribed to higher order reflection, but to different structures in the sample.

In order to investigate the microstructure of the samples, TEM observation on **1/PMMA, 2b/PMMA** and **2c/PMMA** composites at concentration $4.6 \cdot 10^{-2}$M were performed. A representative micrograph of each sample is reported in Figures 12, 13 and 14.

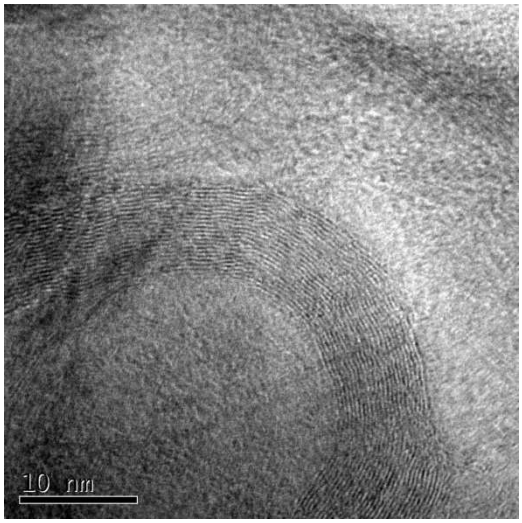

Figure 12. TEM micrograph of **1/PMMA** composite.

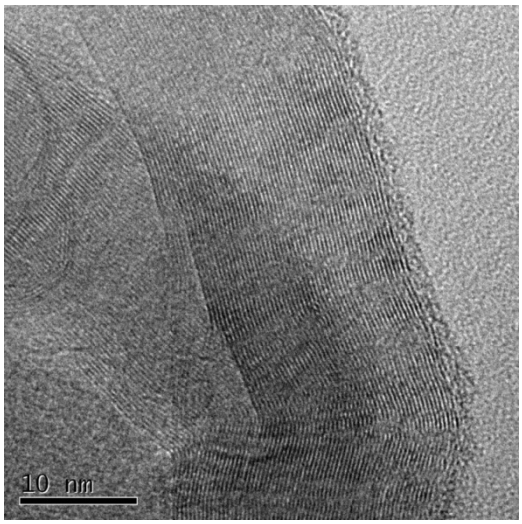

Figure 13. TEM micrograph of **2b/PMMA** composite.

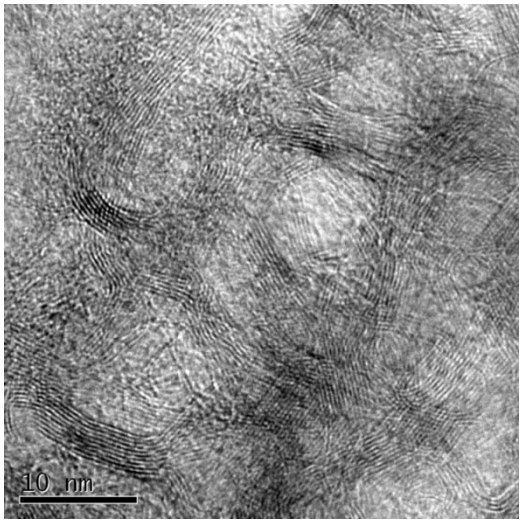

Figure 14. TEM micrograph of **2c/PMMA** composite.

Domains of irregular shape having size in the scale of microns are observed in all investigated samples (see supporting information Figure S8-S10). All these domains show parallel atomic planes whose interplanar distance is about 3.5 Å. This is consistent with graphite interlayer spacing.[51,52] The lateral domains size is roughly 8, 17 and 4.2 nm for the **1/PMMA**, **2b/PMMA** and **2c/PMMA** composites, respectively. The bigger is the lateral domains size the lower is the number of domains.

TEM and SAXS findings suggest that the resulting structure is due to a balance of interactions among the two molecule portions. The wellknown staking tendency of pyrene could be favoured in the composite, thus generating the extended observed structures. The presence of a perfluoroalkyl moiety promotes the formation of large structures as a consequence of repulsive interactions among fluorinated chains and PMMA. The presence of six or more carbon atoms in the fluorinated chain is able to generate fluorocarbon well-defined domains. The interaction among fluorinated chains in **2c** becomes strong enough to overcome the tendency of pyrene stacking and to promote the formation of lamellar structures. Longer homologues (**2c** and **2d**), in addition, promote a crystallization of the polymer as indicated by the appearance of the peak (41 Å) in SAXS data and by some regions observed in TEM micrographs (see supporting information Figure S8-S10).

The thermal stability of the composites has been tested in nitrogen atmosphere by using the TG analysis. Some TGA curves (the residual weight percentage versus temperature) and DTG curves (derivative of the residual weight percentage versus temperature) are reported in supporting information Figure S11.
No char residuals after TGA runs are observed in all samples.
It can be seen that for all composites the thermal decomposition falls to the same values of temperature of pure PMMA.

The DTG curves show clear evidence of the existence of three degradation steps for PMMA which were generally attributed to scissions of head-to-head linkages and at the chain-end initiation from vinylidene ends and to the random internal scission of the polymer chain, respectively.
The decomposition peak in DTG curve at higher temperature (380-400°C) is due to the thermal decomposition of polymer chains.[53]

Conclusions

A set of perfluoroalkyl derivatives of pyrene and new PMMA composite materials, was obtained by exploiting exclusively the photochemical approach.
The performed spectroscopic and structural investigations allowed to obtain complementary information and a clear picture of these interesting materials.
The SAXS data analysis revealed the aggregate formation in dependency of the chain length (C≥8).
The TEM micrographs evidenced the presence of aggregates resulting by π-π stacking tendency and fluorocarbon chain interaction balance. The fluorine content is responsible of the kind of aggregate formation and promotes the crystallization of polymeric matrix.
The study of the emission spectra of the synthesized compounds both in solution and in the polymeric matrix revealed a strong violet-blue emission. The embedding of pyrene perfluoroalkyl derivativesin PMMA produced a shifted stronger emission as further evidenced by the CIE diagram.
The decomposition temperature of the composite materials are comparable to PMMA.
The used synthesis methodology proved to be effective and efficient in order to obtain new materials, and the performed study let us envisage their perspective applications in sensors, fluorescent probes, and optoelectronic devices such as displays, lighting, bio-labels, etc..

Acknowledgements

Authors acknowledge the University of Palermo, FFR 2012-2013 – ATE 0291 “Synthesis and characterization of organic salts as functional ionic phases” and ATE 0594 "Development of new methodologies for the synthesis and functionalization of nanoparticles with luminescence properties for advanced applications".

SAXS and TEM experimental data were provided by C. G. A.-UniNetLab-University of Palermo funded by P.O.R. Sicily 2000-2006, 3.15 / C Q. R..

Thank to Eng. Fulvio Caruso of the University of Palermo, Department of Energy, Information engineering and Mathematical models – DEIM, for the acquisition of points in the CIE chromaticity diagram.

Thank to Dr. Giuseppe Lazzara of the University of Palermo, Department of Physics and Chemistry, for the TGA analysis.

Notes and references

[a] Dipartimento di Scienze e Tecnologie Biologiche, Chimiche e Farmaceutiche, Università degli Studi di Palermo, Viale delle Scienze – Parco d’Orleans II, Ed. 17, I-90128 Palermo, Italy. E-mail: ivana.pibiri@unipa.it
[b] Istituto EuroMediterraneo di Scienza e Tecnologia (IEMEST), Via Emerico Amari 123, 90139, Palermo, Italy.
[c] Consorzio Interuniversitario Nazionale per la Scienza e Tecnologia dei Materiali (INSTM), UdR di Palermo, Viale delle Scienze – Parco d’Orleans II, Ed. 17, I-90128 Palermo, Italy.
[d] Centro Grandi Apparecchiature-UniNetLab, Università di Palermo, Via F. Marini 14, I-90128 Palermo, Italy.

Electronic Supplementary Information (ESI) available: Additional Spectroscopic data and TEM micrographs. See DOI: 10.1039/b000000x/

1 T. M. Figueira-Duarte and K. Mullen, *Chem. Rev.*, 2011, **111**, 7260-7314.
2 K. Kalyanasundaram and J. K. Thomas, *J. Am. Chem. Soc.*, 1977, **99**, 2039-2044.
3 Y. Wang and M. Winnik, *Langmuir*, 1990, **6**, 1437-1439.
4 A. Yekta, B. Xu, J. Buhamel, H. Adiwidjaja and M. Winnik, *Macromolecules*, 1995, **28**, 956-966.
5 W. L. Jia, T. McCormick, Q. D. Liu, H. Fukutani, M. Motala, R. Y. Wang, Y. Tao and S. N. Wang, *J. Mater. Chem.*, 2004, **14**, 3344-3350.
6 H. E. Katz, J. Johnson, A. J. Lovinger and W. Li, *J. Am. Chem. Soc.* 2000, **122**, 7787-7792.
7 J. E. Anthony, *Angew. Chem. Int. Ed.*, 2008, **47**, 452-483.
8 B. A. Jones, M. J. Ahrens, M.-H. Yoon, A. Facchetti, T. J. Marks and M. R. Wasielewski, *Angew. Chem., Int. Ed.*, 2004, **43**, 6363-6366.
9 F. Würthner, P. Osswald, R. Schmidt, T. E. Kaiser, H. Mansikkamäki and M. Könemann, *Org. Lett.*, 2006, **8**, 3765-3768.
10 N. B. Shustova, I. E. Kareev, I. V. Kuvychko, J. B. Whitaker, S. F. Lebedkin, A. A. Popov, L. Dunsch, Y.-S. Chen, K. Seppelt, S. H. Strauss and O. V. Boltalina, *J. Fluorine Chem.*, 2010, **131**, 1198–1212.
11 M. Li, M. Jiang, Y.-X. Zhang and Q. Fang, *Macromolecules*, 1997, **30**, 470-478.
12 Y. Zhang, M. Li, Q. Fang, Y.-X. Zhang, M. Jiang and C. Wu, *Macromolecules*, 1998, **31**, 2527-2532.
13 J. Chen, M. Jiang, Y.-X. Zhang and H. Zhou, *Macromolecules*, 1999, **32**, 4861-4866.
14 S. Buscemi, G. Lazzara, S. Milioto and A. Palumbo Piccionello, *Langmuir*, 2009, **25** *(23)*, 13368–13375.
15 G. Cai, Y. Fu, Y. Li, X. Wan and Z. Shi, *J. Am. Chem. Soc.*, 2007, **129**, 7666-7673.
16 A. E. Shilov and G. B. Shul’pin, *Chem. Rev.*, 1997, **97**, 2879-2932.
17 V. Ritleng, C. Sirlin and M. Pfeffer, *Chem. Rev.*, 2002, **102**, 1731-1769.
18 D. Alberico, M. E. Scott and M. Lautens, *Chem. Rev.* 2007, **107**, 174-238.
19 T. Okazawa, T. Satoh, M. Miura and M. Nomura, *J. Am. Chem.Soc.*, 2002, **124**, 5286-5287.
20 D. R. Stuart and K. Fagnou, *Science*, 2007, **316**, 1172-1175.

21 V. G. Zaitsev and O. Daugulis, *J. Am. Chem. Soc.*, 2005, **127**, 4156-4157.
22 Y. Li, C. Li, W. Yue, W. Jiang, R. Kopecec, J. Qu and Z. Wang, *Org. Lett.*, 2010, **12**, 2374-2377.
23 G. V. D. Tiers, *J. Am. Chem. Soc*., 1960, **82**, 5513.
24 A. Bravo, H. R. Bjørsvik, F. Fontana, L. Liguori, A. Mele and F. Minisci, *J. Org.Chem.*, 1997, **62**, 7128-7136.
25 H. Kimoto, S. Fujii and L. A. Cohen, *J. Org. Chem.*, 1982, **47**, 2867-2872.
26 I. Barroso and J. Gonzalez-Benito, *Polym. Compos.*, 2011, **32**, 1874-1887.
27 T. E. Motaung; M. L. Saladino; A. S. Luyt, D. F. Chillura Martino, *Composites Science and technology*,2012, **73**, 34-39.
28 T. E. Motaung; M. L. Saladino, A. S. Luyt and D. Chillura Martino, *European Polymer Journal*, 2013, **49**, 2022-2030.
29 W. J. Tobler and W. Durisch, *Appl. Energ.*,2008, **85**, 483-493.
30 Y. Zhang, X. Wang, Y. Liu, S. Songa and D. Liu, *J. Mater. Chem.*, 2012, **22**, 11971-11977.
31 T. E. Motaung, A. S. Luyt, M. L. Saladino, D. Chillura Martino and E. Caponetti *eXPRESS Polym. Lett*., 2012, **6**, 871-881.
32 N. Vivona, S. Buscemi, I. Pibiri, A. Palumbo Piccionello and A. Pace, in *Handbook of Synthetic Photochemistry (Eds.: A. Albini, M. Fagnoni), Wiley-VCH, Weinheim*, 2010, pp. 387–416.
33 A. Pace, I. Pibiri, S. Buscemi and N. Vivona, *Heterocycles*, 2004, **63** *(11)*, 2627–2648.
34 S. Buscemi, N. Vivona and T. Caronna, *Synthesis*, 1995, **8**, 917-919.
35 A. Pace, I. Pibiri, S. Buscemi and N. Vivona, *J. Org. Chem.*, 2004, **69**, 4108-4115.
36 A. Palumbo Piccionello, I. Pibiri, A. Pace, R. A. Raccuglia, S. Buscemi, N. Vivona and G. Giorgi, *Heterocycles*, 2007,**71** *(7)*, 1529–1537.
37 S. Buscemi, A. Pace, I. Pibiri, N. Vivona and T. Caronna, *J. Fluorine Chem.*, 2004, **125**, 165-173.
38 S. Buscemi, A. Pace, A. Palumbo Piccionello, I. Pibiri and N. Vivona, *Heterocycles*, 2004, **63**, 1619-1628.
39 M. Bellardita, V. Loddo, G. Palmisano, I. Pibiri, L. Palmisano and V. Augugliaro, *Appl. Catalysis B: Envir.*, 2014, **144**, 607-613.
40 I. Pibiri, A. Palumbo Piccionello, A. Pace, G. Barone and S. Buscemi, *Tetrahedron*, 2013, **69**, 6065-6069.
41 E. Caponetti, M. Leone, V. Militello, V. Pantò, S. Pedone, S. Polizzi and M. L. Saladino, *J. Colloid. Interf. Sci.*, 2005, **284**, 495-500.
42 A. Zanotto, R. Matassa, M. L. Saladino, M. Berrettoni, M. Giorgetti, S. Zamponi and E. Caponetti, *Mater. Chem. Phys.*, 2010, **120**, 118-122.
43 M. L. Saladino, A. Zanotto, D. Chillura Martino, A. Spinella, G. Nasillo and E. Caponetti, *Langmuir*, 2010, **26***(16)*, 13442-13449.
44 D. Wiedenfeld, S. Niyogi and D. Chakrabarti, *J. Fluorine Chem.*, 2000, **104**, 303-306.
45 D. Wiedenfeld, W. Xu and S. Niyogi, *Tetrahedron Lett.*, 2003, **44**, 1579–1582.
46 A. Palumbo Piccionello, A. Guarcello, A. Calabrese, I. Pibiri, A. Pace and S. Buscemi, *Org. Biomol. Chem.*, 2012, **10**, 3044-3052.
47 A. Abate, A. Petrozza, G. Cavallo, G. Lanzani, F. Matteucci, D. W. Bruce, N. Houbenov, P. Metrangolo and G. Resnati, *J. Mater. Chem.*, 2013, **1***(22)*, 6572-6578.
48 F. Lo Celso, I. Pibiri, A. Triolo, R. Triolo, A. Pace, S. Buscemi and N. Vivona, *J. Mat. Chem.*, 2007, **17**, 1201-1208.
49 J. Chen, M. Jiang, Y. Zhang and H. Zhou, *Macromolecules* , 1999, **32** *(15)*, 4861-4866.
50 M. Liu, C. Zhang, W. W. Tjiu, Z. Yang, W. Wang, and T. Liu, *Polymer*, 2013, **54**, 3124-3130.
51 F. Castro-Marcano, R. E. Winans, P. Chupas, K. Chapman, J. M. Calo, J. K. Watson and J. P. Mathews, *Energ. Fuels*, 2012, **26**, 4336–4345.
52 H. Takagi, K. Maruyama, N. Yoshizawa, Y. Yamada and Y. Sato, *Fuel*, 2004, **83**, 2427–2433.
53 T.E. Motaung, A.S. Luyt, F. Bondioli, M. Messori, M.L. Saladino, A. Spinella, G. Nasillo, E. Caponetti, *Polym. Degrad. Stabil.*, 2012, **97**, 1325-1333.